A Generalized Human-In-The-Loop Stability Analysis in the Presence of Uncertain and Redundant Actuator Dynamics

Seyed Shahabaldin Tohidi[1] and Yildiray Yildiz[2]

Abstract— This paper demonstrates the stability limits of a human-in-the-loop closed loop control system, where the plant to be controlled has redundant actuators with uncertain dynamics. The human operator is modeled as a general transfer function, unlike earlier work where specific filters are associated with human reactions. This helps with developing a more general stability analysis, and earlier studies can be considered as special cases of the proposed framework in this paper. Adaptive control allocation is employed to distribute control signals among redundant actuators. A sliding mode controller with a time-varying sliding surface provides desired control inputs to the control allocator. A flight control task, where the pilot controls the pitch angle via a pitch rate stick input is simulated to demonstrate the accuracy of the stability analysis. The Aerodata Model in Research Environment is used as the uncertain, over-actuated aircraft model.

I. INTRODUCTION

Humans' unique skills, such as adaptive behavior in dynamic environments, social interaction and moral judgment capabilities, make them inseparable elements of many control systems. Investigation of human-in-the-loop dynamics help develop safe control mechanisms, and provide a better realization and understanding of human control actions and limitations [1]–[4].

Many studies in the literature focus on developing human models that mimic the human behavior in a specific task. The concept of describing function for human behavior is used by Tustin [5]. Quasi-linear model, proposed by McRuer and Krendel [6] consists of a describing function and a remnant signal accounts for nonlinear behavior. In situations that require very accurate control commands, the human behavior is modeled as a pure gain [7]–[9]. The magnitude of the gain shows human attention level, aggressiveness, or task urgency. Human models with a gain and a pole (lag filter), which captures the humans' limitation of not being able to provide adequate control inputs at high frequencies, are also used for stability analysis [3], [10].

Human reaction delay is a prominent factor in developing human models and a key parameter in stability analysis. The limitations of, for example, the model reference adaptive control in the presence of a human operator with reaction time delay are studied in [1], [11] and [12]. Padé approximation is a useful tool that transforms the delay term to a transfer function, which reduces the complexity of the analysis [13].

In this study, we analyze the stability of human-in-the-loop control systems with redundant actuators assuming that the human reactions can be modeled as a general transfer function.

Actuator redundancy is commonly used in industrial applications to increase system maneuverability, flexibility, safety, and fault tolerability. However, actuator redundancies lead to increased system complexity, which can increase the difficulty of designing appropriate controllers. Control allocators can be used to distribute control signals among redundant actuators [9], [14]–[17], while reducing the complexity of the controller design. Different from the conventional control allocation methods which require fault identification in uncertain systems, adaptive control allocation methods proposed by [18] and [19]–[21] do not require an identification method or assumption on the persistence of excitation of signals. In this paper, the stability of a human-in-the-loop closed loop system in the presence of an adaptive control allocator is analyzed. The plant is assumed to have uncertain redundant actuators and be controlled by a sliding mode controller that feeds the adaptive control allocator with a desired control input vector. Compared to our earlier work [3] that contained simpler human models, e.g. pure gain and lag filter with one pole and no zero, this paper contains a stability analysis with a general transfer function with $\hat{n}$ poles and $\hat{m}$ zeros as the human reaction model. To the best of authors knowledge, human-in-the-loop stability analysis with a general transfer function as the human model in the presence of an adaptive control allocator has not been conducted earlier in the literature.

This paper is organized as follows. Section II presents the over-actuated system dynamics with uncertain actuator effectiveness matrix. Control allocation as well as the sliding mode control design are also presented in this section. Closed loop dynamics including the uncertain plant, control allocation and the controller are given in Section III. Human-in-the-loop stability analysis is provided in Section IV. Simulation results are presented in Section V, and a summary is given in Section VI.

II. PROBLEM SETUP

In this section, we first introduce the dynamics of an over-actuated system in the presence of uncertainty. Then, we describe the adaptive control allocation method. Finally, we overview the sliding mode controller with a time-varying sliding surface to compensate the adaptive control allocation error [22] (see Figure 1).

[1] Seyed Shahabaldin Tohidi is with the Department of Applied Mathematics and Computer Science, Technical University of Denmark, DK-2800 Kgs. Lyngby, Denmark. `sshto@dtu.dk`

[2] Yildiray Yildiz is with Faculty of Mechanical Engineering, Bilkent University, Cankaya, Ankara 06800, Turkey. `yyildiz@bilkent.edu.tr`

A. Over-actuated uncertain plant

Consider the following uncertain over-actuated plant dynamics

$$\dot{x} = Ax + B_u \Lambda u = Ax + B_v B \Lambda u, \tag{1}$$

where $x \in \mathbb{R}^n$ is the system states vector, $u \in \mathbb{R}^m$ is the control input vector, $A \in \mathbb{R}^{n \times n}$ is the known state matrix and $B_u = B_v B \in \mathbb{R}^{n \times m}$ is the known rank deficient control input matrix which is decomposed into the known matrices $B_v \in \mathbb{R}^{n \times \ell}$ and $B \in \mathbb{R}^{\ell \times m}$. The actuator loss of effectiveness is modeled as a diagonal matrix $\Lambda \in \mathbb{R}^{m \times m}$ with unknown positive elements. Throughout the paper, the over-dot notation will be used for time derivatives only, i.e. $(\dot{\cdot}) = d(\cdot)/dt$.

The control allocation objective is to distribute the total control effort $v \in \mathbb{R}^\ell$, produced by an outer loop controller, to the redundant actuators such that

$$B \Lambda u = v \tag{2}$$

is achieved. It is noted that, if this task is achieved perfectly, the system "seen" by the outer loop controller will have the form

$$\dot{x} = Ax + B_v v. \tag{3}$$

Remark 1: The focus of this paper is the human-in-the-loop stability analysis for a control system where control allocation is employed to distribute the total control effort among redundant actuators. In this setting, matrix A being known or not does not effect the development of the control allocation. As seen from (2), only the uncertainty in the input matrix effects the control allocation development. Therefore, to keep the development concise, we will assume that A is known, although the proofs can be extended for an unknown A.

B. Adaptive control allocation

One way to achieve (2) is by using the following control allocation system proposed in [20]

$$\dot{\xi} = A_m \xi + B \Lambda u - v, \tag{4a}$$

$$\dot{\xi}_m = A_m \xi_m, \tag{4b}$$

$$\dot{\theta}_v = \Gamma_\theta \text{Proj}\left(\theta_v, -v e^T P B\right), \tag{4c}$$

$$u = \theta_v^T v, \tag{4d}$$

where $\xi \in \mathbb{R}^r$ is the output of the virtual dynamics, $\theta_v \in \mathbb{R}^{r \times m}$ is the adaptive parameter to be updated, $\xi_m \in \mathbb{R}^r$ is the output of the reference model, $e = \xi - \xi_m$, (4b) is the reference model with a Hurwitz matrix $A_m \in \mathbb{R}^{r \times r}$, (4c) is the adaptive law where the symmetric positive definite matrix P satisfies $A_m^T P + P A_m = -Q$, Q is a symmetric positive definite matrix, $\Gamma_\theta = \gamma_\theta I_\ell$, where γ_θ is a positive scalar, and $\text{Proj}(.,.) : \mathbb{R}^{r \times m} \times \mathbb{R}^{r \times m} \to \mathbb{R}^{r \times m}$ is the projection algorithm [23], [24]. It can be shown that, in the absence of actuator limits, e converges to zero and thus the control allocation goal (2) is achieved [25].
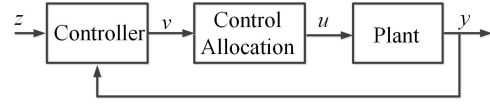
Fig. 1: Closed loop system including control allocation.

C. Outer loop controller

It is required to employ a controller compensating the disturbances originating from the transient dynamics of the control allocation. The sliding mode controller introduced in [22] has the required properties. For the sake of completeness, the main results of the sliding mode controller design is summarized in this section.

From an outer loop controller point of view, the system to be controlled contains the the over-actuated plant (1) and the control allocation, and can be written as

$$\dot{x} = Ax + B_v(I + \Delta B)v, \tag{5}$$

where $\Delta B = B \Lambda \tilde{\theta}_v^T$ is the effect of the control allocation error, and $\tilde{\theta}_v$ is the parameter error defined as $\tilde{\theta}_v \equiv \theta_v - \theta_v^*$, where θ_v^* is the ideal adaptive parameter. It is shown in [20] that the projection algorithm used in the control allocation can be designed such that $||\Delta B|| < 1$. Assume that the dynamics (5) can be written as

$$\begin{bmatrix} \dot{x}^{(1)} \\ \dot{x}^{(2)} \end{bmatrix} = \begin{bmatrix} A_{1,1} & A_{1,2} \\ A_{2,1} & A_{2,2} \end{bmatrix} \begin{bmatrix} x^{(1)} \\ x^{(2)} \end{bmatrix} + B_v(v + d),$$

$$y = C \begin{bmatrix} x^{(1)} \\ x^{(2)} \end{bmatrix}, \tag{6}$$

where $A_{1,1} \in \mathbb{R}^{(n-\ell) \times (n-\ell)}$ is a Hurwitz matrix, $A_{1,2} \in \mathbb{R}^{(n-\ell) \times r}$, $A_{2,1} \in \mathbb{R}^{\ell \times (n-\ell)}$, $A_{2,2} \in \mathbb{R}^{\ell \times \ell}$, $x^{(1)} \in \mathbb{R}^{(n-\ell)}$, $x^{(2)} \in \mathbb{R}^\ell$, $y \in \mathbb{R}^\ell$, $C = [0_{\ell \times (n-\ell)} \ I_\ell]$, $d = \Delta B v$, and $B_v \in \mathbb{R}^{n \times \ell}$ is in the form $[0_{\ell \times (n-\ell)} \ I_\ell]^T$. It is noted that this assumption holds for a large class of open loop unstable aircraft dynamics, and will be shown to hold for the Aerodata Model in Research Environment (ADMIRE) [26] later in the paper in the simulations section.

The sliding surface is given as

$$s\left(x^{(2)}(t), x^{(2)}(t_0), t\right) = x^{(2)}(t) - x^{(2)}(t_0)e^{-\bar{\lambda}(t-t_0)}$$

$$- \frac{2}{\pi} z(t) \tan^{-1}\left(\bar{\lambda}(t - t_0)\right) = 0, \tag{7}$$

where $\bar{\lambda} > 0$ is a scalar parameter, $x^{(1)} \in \mathbb{R}^{(n-\ell)}$ and $x^{(2)} \in \mathbb{R}^\ell$ are defined in (6), $s \in \mathbb{R}^\ell$ is the sliding surface, and $z(t) \in \mathbb{R}^\ell$ is the reference to be tracked. It is proved in [22] that when $x^{(2)}(t)$ is on the sliding surface (7), $x^{(1)}(t)$ and $x^{(2)}(t)$ are bounded for all $t \geq t_0$ and $\lim_{t \to \infty} y(t) = z(t)$.

Definition 1: $\text{sign}_v(a)$, where a is a column vector, is a diagonal matrix whose elements are the signs of the elements of the vector a. For example, $\text{sign}_v([a_1 \ a_2]^T) = \text{diag}(\text{sign}(a_1), \text{sign}(a_2))$, where a_1 and a_2 are scalars.

Consider the dynamics given by (6), and the sliding surface (7). It can be shown that the trajectories of $x^{(2)}$

660

start, at $t = t_0$, on the sliding surface (7), and stay there if the control law

$$v(t) = - A_{2,1}x^{(1)}(t) - A_{2,2}x^{(2)}(t) - \bar{\lambda}x^{(2)}(0)e^{-\bar{\lambda}t}$$
$$+ \frac{2}{\pi}\dot{z}(t)\tan^{-1}(\bar{\lambda}t) + \frac{2}{\pi}z(t)\frac{\bar{\lambda}}{1+\bar{\lambda}^2t^2}$$
$$- \text{sign}_v\left(s(x^{(2)}(t), x^{(2)}(0), t)\right)\rho, \qquad (8)$$

is implemented, where $\rho \in R^\ell$ contains the upper bounds on the absolute values of the elements of the disturbance vector d and $\text{sign}_v(.) : \mathbb{R}^n \to \mathbb{R}^{n\times n}$ is defined in Definition 1. Note that the trajectories of $x^{(2)}$ are on the sliding surface (7) at $t = t_0$. Thus, by omitting the reaching phase, the trajectories are always in the sliding phase, which guarantees the robustness of the controller.

The closed loop system including the over-actuated plant, adaptive control allocation and the sliding mode controller is introduced in this section (see Figure 1). In the sequel, the effect of human dynamics on the stability of the closed loop system is analyzed.

III. HUMAN OPERATOR POINT OF VIEW: NONLINEAR TIME-VARYING DYNAMICS

The system to be controlled by the human operator contains the uncertain over-actuated plant, adaptive control allocation and the sliding mode controller introduced in Section II. Although the plant is linear time invariant, the existence of the adaptive control allocator and the sliding mode controller leads to a nonlinear time-varying closed loop system.

Substituting (8) into (6), the nonlinear time-varying system dynamics can be obtained as

$$\begin{cases} \dot{x}^{(1)}(t) = A_{1,1}x^{(1)}(t) + A_{1,2}x^{(2)}(t), \\[2mm] \dot{x}^{(2)}(t) = -\bar{\lambda}x^{(2)}(0)e^{-\bar{\lambda}t} + \frac{2}{\pi}\dot{z}(t)\tan^{-1}(\bar{\lambda}t) + d(t) \\[2mm] \qquad + \frac{2}{\pi}z(t)\frac{\bar{\lambda}}{1+\bar{\lambda}^2t^2} - \text{sign}_v\left(s\left(x^{(2)}(t), x^{(2)}(0), t\right)\right)\rho, \\[2mm] y(t) = x^{(2)}(t). \end{cases}$$
$$(9)$$

ADMIRE [26], which is an over-actuated aircraft model, is utilized as the plant to be controlled. The model can be written in the form of (6), with $x^{(1)} = [\alpha \ \beta]^T$ and $x^{(2)} = [p \ q \ r]^T$, where α, β, p, q and r are the angle of attack, sideslip angle, roll rate, pitch rate and yaw rate, respectively. Also, the reference signal, $z(t)$, is taken as $z = [p_d, \ q_d, \ r_d]^T$, where p_d, q_d and r_d are the desired roll, pitch and yaw rates,
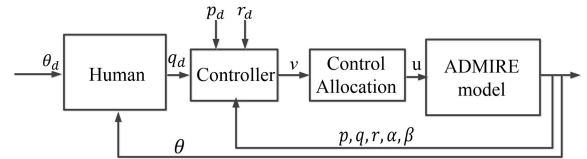
Fig. 2: The evolution of states considering different human operator models.

respectively. Therefore, (9) can be written as

$$\begin{bmatrix} \dot{\alpha}(t) \\ \dot{\beta}(t) \end{bmatrix} = A_{1,1}\begin{bmatrix} \alpha(t) \\ \beta(t) \end{bmatrix} + A_{1,2}\begin{bmatrix} p(t) \\ q(t) \\ r(t) \end{bmatrix}, \qquad (10)$$

$$\begin{bmatrix} \dot{p}(t) \\ \dot{q}(t) \\ \dot{r}(t) \end{bmatrix} = -\bar{\lambda}e^{-\bar{\lambda}t}\begin{bmatrix} p(0) \\ q(0) \\ r(0) \end{bmatrix} + \frac{2}{\pi}\tan^{-1}(\bar{\lambda}t)\begin{bmatrix} \dot{p}_d(t) \\ \dot{q}_d(t) \\ \dot{r}_d(t) \end{bmatrix}$$
$$+ \frac{2}{\pi}\frac{\bar{\lambda}}{1+\bar{\lambda}^2t^2}\begin{bmatrix} p_d(t) \\ q_d(t) \\ r_d(t) \end{bmatrix} - \text{sign}_v(s)\rho + d(t), \quad (11)$$

$$y(t) = [p(t) \ q(t) \ r(t)]^T, \qquad (12)$$

where the arguments of $s\left(x(2)(t); x(2)(t); t\right)$ are dropped for clarity.

IV. HUMAN-IN-THE-LOOP STABILITY ANALYSIS

In Section II, it is shown that the control signal (8) keeps the trajectories of $p(t)$, $q(t)$ and $r(t)$ on the sliding surface (7) for all $t \geq t_0$. Furthermore, on the sliding surface (7), $p(t)$, $q(t)$ and $r(t)$ remain bounded and track their references $p_d(t)$, $q_d(t)$ and $r_d(t)$, assuming that the references are bounded. Therefore, using (10) it can be concluded that $\alpha(t)$ and $\beta(t)$ remain bounded, given that $p(t)$, $q(t)$ and $r(t)$ are bounded. In this section, we integrate the pilot in the control system and analyze the stability of the overall human-in-the-loop closed loop dynamics. The resulting control structure is shown in Figure 2.

Remark 2: It is noted that in the following analysis, although the references $p_d(t)$ and $r_d(t)$ are assumed to be bounded, it will not be assumed that $q_d(t)$ is also bounded. Therefore, the boundedness of $q(t)$, $\alpha(t)$ and $\beta(t)$ need to be shown.

Consider the transfer function

$$\frac{q_d(s)}{\theta_d(s) - \theta(s)} = \frac{b_m s^{\hat{m}} + b_{m-1}s^{\hat{m}-1} + ... + b_0}{s^{\hat{n}} + a_{n-1}s^{\hat{n}-1} + ... + a_0}, \qquad (13)$$

as the human operator model, where $\hat{m}$ and $\hat{n}$ are integers such that $\hat{n} > 0$, $\hat{m} \geq 0$ and $\hat{m} \leq \hat{n}$, and a_i and b_j for $i = 0, ..., \hat{n} - 1$ and $j = 0, ..., \hat{m}$, are real constants. The transfer function (13) can be represented in the minimal state space form as

$$\dot{x}_h(t) = A_h x_h(t) + B_h\left(\theta_d(t) - \theta(t)\right), \qquad (14)$$
$$q_d(t) = C_h x_h(t) + D_h\left(\theta_d(t) - \theta(t)\right), \qquad (15)$$

where $x_h \in \mathbb{R}^{\hat{n}}$ is the vector containing the states of the human model, $A_h \in \mathbb{R}^{\hat{n}\times\hat{n}}$, $B_h \in \mathbb{R}^{\hat{n}}$, $C_h \in \mathbb{R}^{1\times\hat{n}}$ and

$D_h \in \mathbb{R}$ are constant matrices, $q_d \in \mathbb{R}$ is the output of the human model and also the pitch rate reference for the controller (see Figure 2), $\theta_d \in \mathbb{R}$ is the desired pitch angle and $\theta \in \mathbb{R}$ is the measured pitch angle.

Using (7), where $x^{(2)} = [p \; q \; r]^T$, the trajectory of $q(t)$ on the sliding surface can be found. Considering small angles, we have $\dot{\theta}(t) = q(t)$, and using (15), the pitch angle dynamics can be written as

$$\dot{\theta}(t) = q(0)e^{-\bar{\lambda}t} + \frac{2}{\pi}tan^{-1}(\bar{\lambda}t)C_h x_h(t)$$
$$+ \frac{2}{\pi}tan^{-1}(\bar{\lambda}t)D_h\left(\theta_d(t) - \theta(t)\right). \quad (16)$$

Augmenting the dynamics of general human model (14) and pitch angle (16), we have

$$\begin{bmatrix} \dot{\theta}(t) \\ \dot{x}_h(t) \end{bmatrix} = \underbrace{\begin{bmatrix} -\frac{2}{\pi}tan^{-1}(\bar{\lambda}t)D_h & \frac{2}{\pi}tan^{-1}(\bar{\lambda}t)C_h \\ -B_h & A_h \end{bmatrix}}_{\bar{A}(t)} \underbrace{\begin{bmatrix} \theta(t) \\ x_h(t) \end{bmatrix}}_{\bar{x}(t)}$$
$$+ \underbrace{\begin{bmatrix} \frac{2}{\pi}tan^{-1}(\bar{\lambda}t)D_h \\ B_h \end{bmatrix}}_{\bar{B}} \theta_d(t) + \underbrace{\begin{bmatrix} q(0)e^{-\bar{\lambda}t} \\ 0 \end{bmatrix}}_{\omega(t)}. \quad (17)$$

By defining $\bar{x}(t) = [\theta(t) \; x_h^T(t)]^T$, (17) can be written in the following compact form

$$\dot{\bar{x}}(t) = \bar{A}(t)\bar{x}(t) + \bar{B}\theta_d(t) + \omega(t). \quad (18)$$

In the following, the stability of (18) is investigated. At first, we analyze the stability of $\dot{\bar{x}}(t) = \bar{A}(t)\bar{x}(t)$ and then explore the conditions for the stability of (18), which concludes the stability of human-in-the-loop closed loop system.

Theorem 1: The time-varying system $\dot{\bar{x}}(t) = \bar{A}(t)\bar{x}(t)$, where $\bar{A}(t)$ and $\bar{x}(t)$ are given in (17), is uniformly exponentially stable if

$$\lambda_i\left(\begin{bmatrix} -D_h & C_h \\ -B_h & A_h \end{bmatrix}\right) \in \mathbb{C}^-, \quad i = 1, ..., \hat{n}+1, \quad (19)$$

where $\lambda_i(.)$ provides ith eigenvalue of the matrix.

Proof: The time-varying matrix $\bar{A}(t)$ can be written as

$$\bar{A}(t) = \underbrace{\begin{bmatrix} -D_h & C_h \\ -B_h & A_h \end{bmatrix}}_{\bar{A}_1}$$
$$+ \underbrace{\begin{bmatrix} \left(-\frac{2}{\pi}tan^{-1}(\bar{\lambda}t) + 1\right)D_h & \left(\frac{2}{\pi}tan^{-1}(\bar{\lambda}t) - 1\right)C_h \\ 0 & 0 \end{bmatrix}}_{\bar{A}_2(t)}.$$
$$(20)$$

If all of the eigenvalues of $\bar{A}_1$ are in $\mathbb{C}^-$, then the origin of the differential equation $\dot{\bar{x}}(t) = \bar{A}_1\bar{x}(t)$ is exponentially stable. Thus, there exist a scalar function $\bar{V}(x)$ satisfying [27]

$$\bar{c}_1||\bar{x}||^2 \leq \bar{V} \leq \bar{c}_2||\bar{x}||^2 \quad (21)$$
$$\frac{d\bar{V}}{d\bar{x}}\bar{A}_1\bar{x}(t) \leq -\bar{c}_3||\bar{x}||^2 \quad (22)$$
$$||\frac{d\bar{V}}{d\bar{x}}|| \leq \bar{c}_4||\bar{x}||, \quad (23)$$

where $\bar{c}_1$, $\bar{c}_2$, $\bar{c}_3$ and $\bar{c}_4$ are positive constants. Considering the system $\dot{\bar{x}}(t) = \bar{A}(t)\bar{x}(t) = \bar{A}_1\bar{x}(t) + \bar{A}_2(t)\bar{x}(t)$ and using (21)-(23), an upper bound on the time derivative of $\bar{V}$ can be obtained as

$$\dot{\bar{V}} = \frac{d\bar{V}}{d\bar{x}}\bar{A}_1\bar{x}(t) + \frac{d\bar{V}}{d\bar{x}}\bar{A}_2(t)\bar{x}(t)$$
$$\leq -\bar{c}_3||\bar{x}||^2 + \bar{c}_4\bar{c}_5\left|\frac{2}{\pi}tan^{-1}(\bar{\lambda}t) - 1\right|||\bar{x}||^2$$
$$\leq -\frac{\bar{c}_3}{\bar{c}_2}\bar{V} + \frac{\bar{c}_4\bar{c}_5}{\bar{c}_1}\left|\frac{2}{\pi}tan^{-1}(\bar{\lambda}t) - 1\right|\bar{V}$$
$$= -\left(\frac{\bar{c}_3}{\bar{c}_2} - \frac{\bar{c}_4\bar{c}_5}{\bar{c}_1}\left|\frac{2}{\pi}tan^{-1}(\bar{\lambda}t) - 1\right|\right)\bar{V}, \quad (24)$$

where $\bar{c}_5 = (||D_h||^2 + ||C_h||^2)^{1/2}$. Using the comparison lemma [27], we get

$$\bar{V} \leq e^{-(\frac{\bar{c}_3}{\bar{c}_2}t - \frac{\bar{c}_4\bar{c}_5}{\bar{c}_1}\int_0^t|\frac{2}{\pi}tan^{-1}(\bar{\lambda}\tau) - 1|d\tau)}\bar{V}(\hat{x}(0)). \quad (25)$$

Using (21), (25) can be written as

$$||\bar{x}(t)||^2 \leq \frac{\bar{c}_2}{\bar{c}_1}e^{-(\frac{\bar{c}_3}{\bar{c}_2}t - \frac{\bar{c}_4\bar{c}_5}{\bar{c}_1}\int_0^t|\frac{2}{\pi}tan^{-1}(\bar{\lambda}\tau) - 1|d\tau)}||\bar{x}(0)||^2, \quad (26)$$

which leads to

$$||\bar{x}(t)|| \leq \sqrt{\frac{\bar{c}_2}{\bar{c}_1}}e^{-(\frac{\bar{c}_3}{2\bar{c}_2}t - \frac{\bar{c}_4\bar{c}_5}{2\bar{c}_1}\int_0^t|\frac{2}{\pi}tan^{-1}(\bar{\lambda}\tau) - 1|d\tau)}||\bar{x}(0)||. \quad (27)$$

Let $\gamma(t) = |\frac{2}{\pi}tan^{-1}(\bar{\lambda}t) - 1|$, it should be noted that $\gamma(t) \geq 0$ and $\lim_{t\to\infty}\gamma(t) = 0$. Also, the time derivative of $\gamma(t)$ is bounded for $\forall t \geq 0$, and $\frac{d}{dt}\gamma(t) = \frac{-2\bar{\lambda}}{\pi(1+\bar{\lambda}^2t^2)} < 0$. Therefore, there exist positive constants $\bar{T}$ and $\bar{\epsilon}$ such that $\gamma(t) \leq \bar{\epsilon} < \frac{\bar{c}_3\bar{c}_1}{\bar{c}_2\bar{c}_4\bar{c}_5}, \forall t \geq \bar{T}$. Also, from the boundedness of $\gamma(t)$ we have $\int_0^{\bar{T}}\gamma(t) = \bar{\eta}$, where $\bar{\eta}$ is a positive constant. The following two cases should be considered: **(1)** For $t \leq \bar{T}$, $\int_0^t\gamma(\tau)d\tau \leq \bar{\eta}$. Thus, using (27), an upper bound for $||\bar{x}||$ can be obtained as

$$||\bar{x}(t)|| \leq \sqrt{\frac{\bar{c}_2}{\bar{c}_1}}\bar{\kappa}e^{-(\frac{\bar{c}_3}{2\bar{c}_2}t)}||\bar{x}(0)||, \quad (28)$$

where $\bar{\kappa} = e^{\frac{\bar{c}_4\bar{c}_5}{2\bar{c}_1}\bar{\eta}}$. **(2)** For $t > \bar{T}$, $\int_0^t\gamma(\tau)d\tau = \int_0^{\bar{T}}\gamma(\tau)d\tau + \int_{\bar{T}}^t\gamma(\tau)d\tau \leq \bar{\epsilon}t + \bar{\eta}$. Substituting this result in (27), an upper bound for $||\bar{x}||$ can be obtained as

$$||\bar{x}(t)|| \leq \sqrt{\frac{\bar{c}_2}{\bar{c}_1}}\bar{\kappa}e^{-(\frac{\bar{c}_3}{2\bar{c}_2}t - \frac{\bar{c}_4\bar{c}_5}{2\bar{c}_1}\bar{\epsilon}t)}||\bar{x}(0)|| \quad (29)$$

Since $\bar{\epsilon} < \frac{\bar{c}_3\bar{c}_1}{\bar{c}_2\bar{c}_4\bar{c}_5}$, the origin of $\dot{\bar{x}}(t) = \bar{A}(t)\bar{x}(t)$ is exponentially stable. ∎

Theorem 2: The solution of the linear time-varying system (18), where $\bar{A}(t)$, $\bar{B}$, $\omega(t)$ and $\bar{x}(t)$ are given in (17), is bounded if

$$\lambda_i\left(\begin{bmatrix} -D_h & C_h \\ -B_h & A_h \end{bmatrix}\right) \in \mathbb{C}^-, \quad i = 1, ..., \hat{n}+1. \quad (30)$$

Proof: The solution of the system (18) is

$$\bar{x}(t) = \bar{\Phi}(t, t_0)\bar{x}(t_0) + \int_{t_0}^t \bar{\Phi}(t, \tau)(\bar{B}\theta_d(\tau) + \omega(\tau)), \quad (31)$$

662

where $\bar{\Phi}(t, t_0)$ is the state transition matrix. By using the definitions of $\bar{B}$ and $\omega(t)$ given in (17), it can be obtained that $\sup_{0 \leq \tau \leq t} ||\bar{B}\theta_d(\tau) + \omega(\tau)|| = ||\bar{B}||\theta_{d_{max}} + |q(0)|$. Also, it is proved in Theorem 1 that if $\lambda_i(\bar{A}_1) \in \mathbb{C}^-$, $i = 1, ..., \hat{n} + 1$, the origin of $\dot{\bar{x}}(t) = \bar{A}(t)\bar{x}(t)$ is exponentially stable, that is, there exist finite positive constants $\bar{k}_1$ and $\bar{k}_2$ such that $||\bar{\Phi}(t, t_0)|| \leq \bar{k}_1 e^{-\bar{k}_2(t - t_0)}$, for $\forall t \geq t_0$. Therefore, considering $t_0 = 0$, an upper bound on $||\bar{x}(t)||$ can be obtained as

$$
\begin{aligned}
||\bar{x}(t)|| &\leq \bar{k}_1 e^{-\bar{k}_2 t} |\bar{x}(0)| + \bar{k}_1(||\bar{B}||\theta_{d_{max}} + |q(0)|) \\
&\quad \times \int_0^t e^{-\bar{k}_2(t - \tau)} d\tau \\
&= \bar{k}_1 e^{-\bar{k}_2 t} |\bar{x}(0)| + \frac{\bar{k}_1}{\bar{k}_2}(||\bar{B}||\theta_{d_{max}} + |q(0)|) \\
&\quad \times (1 - e^{-\bar{k}_2 t}) \\
&\leq \bar{k}_1 |\bar{x}(0)| + \frac{\bar{k}_1}{\bar{k}_2}(||\bar{B}||\theta_{d_{max}} + |q(0)|). \quad (32)
\end{aligned}
$$

Therefore, $\theta(t)$ and $x_h(t)$ are bounded. Assuming that $\theta_d(t)$ is bounded, the boundedness of $\theta(t)$ proves that $e_\theta(t) = \theta_d(t) - \theta(t)$ is bounded as well. ∎

Remark 3: In addition to the stability, performance of the closed loop system can also be analyzed. One of the performance metrics is the upper bound of the norm of the tracking error $e_\theta(t) = \theta_d(t) - \theta(t)$. Using (32), we can obtain this bound as

$$
\begin{aligned}
||e_\theta(t)|| &= ||\theta_d(t) - \theta(t)|| \\
&\leq ||\theta_d(t)|| + ||\theta(t)|| \\
&\leq ||\theta_d(t)|| + ||\bar{x}(t)|| \\
&= ||\theta_d(t)|| + \bar{k}_1 |\bar{x}(0)| + \frac{\bar{k}_1}{\bar{k}_2}(||\bar{B}||\theta_{d_{max}} + |q(0)|).
\end{aligned}
$$
(33)

Remark 4: Different state space representations of (13) do not change the analysis provided in Theorems 1 and 2. To show this, consider the state space representation

$$
\dot{x}_h(t) = T_x^{-1} A_h T_x x_h(t) + T_x^{-1} B_h(\theta_d(t) - \theta(t)), \quad (34)
$$

$$
q_d(t) = C_h T_x x_h(t) + D_h(\theta_d(t) - \theta(t)), \quad (35)
$$

where T_x is the linear transformation matrix. Let $M = \begin{bmatrix} -D_h & C_h \\ -B_h & A_h \end{bmatrix}$ and $M_T = \begin{bmatrix} -D_h & C_h T_x \\ -T_x^{-1} B_h & T_x^{-1} A_h T_x \end{bmatrix}$, where M_T can be written as

$$
M_T = \begin{bmatrix} I & 0 \\ 0 & T_x^{-1} \end{bmatrix} M \begin{bmatrix} I & 0 \\ 0 & T_x \end{bmatrix}. \quad (36)
$$

By defining $\bar{T}_x = \begin{bmatrix} I & 0 \\ 0 & T_x \end{bmatrix}$, we have

$$
\begin{aligned}
det(sI - M_T) &= det(sI - \bar{T}_x^{-1} M \bar{T}_x) \\
&= det(\bar{T}_x^{-1}(sI - M)\bar{T}_x) \\
&= det(\bar{T}_x^{-1}) det(sI - M) det(\bar{T}_x) \\
&= det(sI - M), \quad (37)
\end{aligned}
$$

where $det(.)$ stands for the determinant of a matrix.

V. APPLICATION EXAMPLE

A. ADMIRE Model

The ADMIRE [26], which is an over-actuated aircraft model, is utilized for the simulations. The linearized model at Mach 0.22 and altitude 3000 m is given as

$$
\begin{aligned}
\dot{x} &= Ax + B_u u = Ax + B_v v, \\
v &= Bu, \quad B_u = B_v B, \quad B_v = [0_{3\times2} \ I_{3\times3}]^T, \\
x &= [\alpha \ \beta \ p \ q \ r]^T, \quad y = [p \ q \ r]^T, \quad u = [u_c \ u_{re} \ u_{le} \ u_r]^T,
\end{aligned}
$$
(38)

where the states α, β, p, q and r are the angle of attack, sideslip angle, roll rate, pitch rate and yaw rate, respectively. The vector u includes u_c, u_{re}, u_{le} and u_r, which are the commanded deflections of the canard wings, right and left elevons, and the rudder deflection, respectively. The state and control matrices, A and B_u, can be found in [26], and omitted here for brevity. To introduce the actuator effectiveness uncertainty, we modify the model (38) as

$$
\begin{aligned}
\dot{x} &= Ax + B_u \Lambda u \\
&= Ax + B_v B \Lambda u, \quad (39)
\end{aligned}
$$

where $\Lambda \in \mathbb{R}^{4\times4}$ is a diagonal matrix with uncertain positive elements. Substituting the allocated signal u given by (4d), and using $\theta_v^T = \theta_v^{*T} + \tilde{\theta}_v^T$, (39) can be written as

$$
\begin{aligned}
\dot{x} &= Ax + B_v B \Lambda \theta_v^T v \\
&= Ax + B_v(I + B\Lambda\tilde{\theta}_v^T)v, \quad (40)
\end{aligned}
$$

which is in the proper form for the controller design (5).

B. Simulation Results

The closed loop control structure depicted in Figure 2 is used for the simulations. The reference signals, $p_d(t)$, $q_d(t)$ and $r_d(t)$ are roll, pitch and yaw rate references, respectively. The signals $p_d(t)$ and $r_d(t)$ are provided to the controller externally, and $q_d(t)$ is the human operator command. The effectiveness of the actuators are reduced by 30% at $t = 7$s.

The poles of the matrix $\begin{bmatrix} -D_h & C_h \\ -B_h & A_h \end{bmatrix}$ for the various human transfer function models, denoted as TF1, ..., TF6, are provided in Table I. Using Theorem 2 and the results provided in Table I, it can be predicted that the closed loop system trajectories will be bounded for transfer functions TF1, TF2, TF5 and TF6. Figure 3 illustrates the evolution of the state trajectories. It is seen that the states remain bounded for TF1, TF2, TF5 and TF6, and unbounded for models TF3 and TF4. These results are consistent with Theorem 2.

VI. SUMMARY

The stability limits of a human-in-the-loop closed loop control system for a human operator reaction model that is represented as a general transfer function are analyzed in the presence of uncertain redundant actuators. A sliding mode controller is used to guarantee reference tracking and boundedness of the states, when the controller receives bounded references. The adaptive control allocation is employed to distribute the total control signal vector among the redundant uncertain actuators. The simulations performed using different operator models agree with the stability analysis.

663

TABLE I

	Human transfer function	$\lambda_i \left(\begin{bmatrix} -D_h & C_h \\ -B_h & A_h \end{bmatrix} \right)$
TF1	$\frac{10}{s+10}$	$-1.127, -8.873$
TF2	$\frac{s+1}{(s+2)(s+3)}$	$-0.16, -2.4 \pm 0.6j$
TF3	$\frac{s+1}{(s-2)(s+3)}$	$1.655, 0.21, -2.86$
TF4	$\frac{s-1}{(s+2)(s+3)}$	$0.13, -2.5 \pm 1.04j$
TF5	$\frac{(s+1)(s+2)}{(s+3)(s+4)}$	$-0.144, -2.678, -5.177$
TF6	$\frac{(s+1)(s+2)}{(s+3)(s+4)(s+5)}$	$-0.03, -2.8, -4.6 \pm 0.96j$
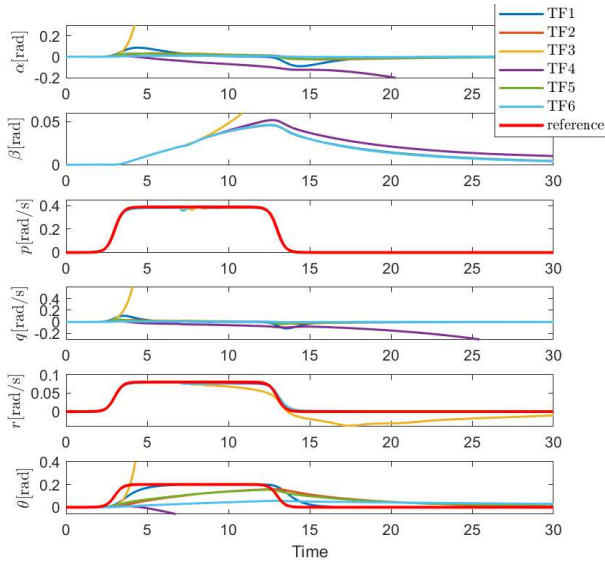
Fig. 3: The evolution of states considering different human operator models.

REFERENCES

[1] T. Yucelen, Y. Yildiz, R. Sipahi, E. Yousefi, and N. Nguyen, "Stability limit of human-in-the-loop model reference adaptive control architectures," *International Journal of Control*, vol. 91, pp. 2314–2331, 2018.

[2] M. Xia, A. Rahnama, S. Wang, and P. J. Antsaklis, "On guaranteeing passivity and performance with a human controller," in *Mediterranean Conference on Control and Automation (MED)*, pp. 722–727, IEEE, 2015.

[3] S. Tohidi and Y. Yildiz, "Adaptive control allocation: A human-in-the-loop stability analysis," *IFAC-PapersOnLine*, vol. 53, no. 2, pp. 6321–6326, 2020.

[4] S. S. Tohidi and Y. Yildiz, "A control theoretical adaptive human pilot model: Theory and experimental validation," *IEEE Transactions on Control Systems Technology*, accepted for publication, 2022.

[5] A. Tustin, "The nature of the operator response in manual control, and its implications for controller design," *Journal of the Institution of Electrical Engineers-Part IIA: Automatic Regulators and Servo Mechanisms*, vol. 94, no. 2, pp. 190–206, 1947.

[6] D. T. McRuer and E. S. Krendel, "Dynamic response of human operators," tech. rep., WADC-TR-56-524, 1957.

[7] D. McRuer, D. Klyde, and T. Myers, "Development of a comprehensive pio theory," in *Atmospheric Flight Mechanics Conference*, p. 3433, 1996.

[8] D. Klyde and D. Mitchell, "A pio case study-lessons learned through analysis," in *AIAA Atmospheric Flight Mechanics Conference and Exhibit*, p. 5813, 2005.

[9] Y. Yildiz and I. Kolmanovsky, "Stability properties and cross coupling performance of the control allocation scheme CAPIO," *Journal of Guidance, Control, and Dynamics*, vol. 34, pp. 1190–1196, 2011.

[10] M. R. Anderson, "Pilot induced oscillations involving multiple nonlinearities," *Journal of Guidance, Control, and Dynamics*, vol. 21, no. 5, pp. 786–791, 1998.

[11] E. Yousefi, Y. Yildiz, R. Sipahi, and T. Yucelen, "Stability analysis of a human-in-the-loop telerobotics system with two independent time-delays," *IFAC-PapersOnLine*, vol. 50, no. 1, pp. 6519–6524, 2017.

[12] E. Arabi, T. Yucelen, R. Sipahi, and Y. Yildiz, "Human-in-the-loop systems with inner and outer feedback control loops: Adaptation, stability conditions, and performance constraints," in *AIAA Scitech Forum*, 2019.

[13] S.-C. Tsay, I. LONG WU, and T.-T. Lee, "Optimal control of linear time-delay systems via general orthogonal polynomials," 1988.

[14] T. A. Johansen and T. I. Fossen, "Control allocation—a survey," *Automatica*, vol. 49, no. 5, pp. 1087–1103, 2013.

[15] W. C. Durham, "Constrained control allocation," *Journal of Guidance, Control, and Dynamics*, pp. 717–725, 1993.

[16] J. A. M. Petersen and M. Bodson, "Constrained quadratic programming techniques for control allocation," *IEEE Transactions on Control Systems Technology*, vol. 14, no. 1, pp. 91–98, 2006.

[17] S. S. Tohidi, A. Khaki Sedigh, and D. Buzorgnia, "Fault tolerant control design using adaptive control allocation based on the pseudo inverse along the null space," *International Journal of Robust and Nonlinear Control*, vol. 26, no. 16, pp. 3541–3557, 2016.

[18] J. Tjønnås and T. A. Johansen, "Adaptive control allocation," *Automatica*, vol. 44, no. 11, pp. 2754–2765, 2008.

[19] G. P. Falconí and F. Holzapfel, "Adaptive fault tolerant control allocation for a hexacopter system," in *American Control Conference (ACC), 2016*, pp. 6760–6766, IEEE, 2016.

[20] S. S. Tohidi, Y. Yildiz, and I. Kolmanovsky, "Adaptive control allocation for constrained systems," *Automatica*, vol. 121, p. 109161, 2020.

[21] S. S. Tohidi and Y. Yildiz, "Discrete adaptive control allocation," in *American Control Conference (ACC)*, pp. 3731–3736, IEEE, 2021.

[22] S. Tohidi, Y. Yildiz, and I. Kolmanovsky, "Sliding mode control for over-actuated systems with adaptive control allocation and its applications to flight control," in *IEEE Conference on Control Technology and Applications (CCTA)*, pp. 765–770, IEEE, 2021.

[23] E. Lavretsky and K. Wise, "Robust and adaptive control: With aerospace applications," 2013.

[24] S. S. Tohidi and Y. Yildiz, "Handling actuator magnitude and rate saturation in uncertain overactuated systems: A modified projection algorithm approach," *International Journal of Control*, pp. 1–14, 2020.

[25] S. S. Tohidi, Y. Yildiz, and I. Kolmanovsky, "Fault tolerant control for over-actuated systems: an adaptive correction approach," in *American Control Conference (ACC), 2016*, pp. 2530–2535, IEEE, 2016.

[26] O. Härkegård and S. T. Glad, "Resolving actuator redundancy—optimal control vs. control allocation," *Automatica*, vol. 41, no. 1, pp. 137–144, 2005.

[27] H. K. Khalil, *Nonlinear systems*. Upper Saddle River, 2002.